Cell

Nuclear Aggregation of Olfactory Receptor Genes Governs Their Monogenic Expression

E. Josephine Clowney,[1] Mark A. LeGros,[2,4] Colleen P. Mosley,[2] Fiona G. Clowney,[2] Eirene C. Markenskoff-Papadimitriou,[3] Markko Myllys,[5] Gilad Barnea,[6] Carolyn A. Larabell,[2,4] and Stavros Lomvardas[1,2,3,*]

[1]Program in Biomedical Sciences
[2]Department of Anatomy
[3]Program in Neurosciences
University of California, San Francisco, San Francisco, CA 94158, USA
[4]Physical Biosciences Division, Lawrence Berkeley National Laboratory, Berkeley, CA 94720, USA
[5]Department of Physics, University of Jyväskylä, Jyväskylä FI-40014, Finland
[6]Department of Neuroscience, Brown University, Providence, RI 02912, USA
*Correspondence: stavros.lomvardas@ucsf.edu
http://dx.doi.org/10.1016/j.cell.2012.09.043

SUMMARY

Gene positioning and regulation of nuclear architecture are thought to influence gene expression. Here, we show that, in mouse olfactory neurons, silent olfactory receptor (OR) genes from different chromosomes converge in a small number of heterochromatic foci. These foci are OR exclusive and form in a cell-type-specific and differentiation-dependent manner. The aggregation of OR genes is developmentally synchronous with the downregulation of lamin b receptor (LBR) and can be reversed by ectopic expression of LBR in mature olfactory neurons. LBR-induced reorganization of nuclear architecture and disruption of OR aggregates perturbs the singularity of OR transcription and disrupts the targeting specificity of the olfactory neurons. Our observations propose spatial sequestering of heterochromatinized OR family members as a basis of monogenic and monoallelic gene expression.

INTRODUCTION

Spatial compartmentalization of genes in the mammalian nucleus is believed to serve regulatory purposes (Fraser and Bickmore, 2007). Heterochromatin and euchromatin were originally cytological descriptions of silent and active regions of the genome and were only later biochemically characterized (Zacharias, 1995). In most cell types, interactions with the nuclear lamina locate heterochromatin at the periphery of the nucleus, and euchromatin occupies the nuclear core (Peric-Hupkes and van Steensel, 2010). Higher-resolution views of the nucleus reveal additional levels of organization and compartmentalization. For example, transcription may be restricted to specialized nuclear regions or transcription factories where genes converge in a nonrandom fashion (Eskiw et al., 2010). Finally, inter- and intragenic interactions over large genomic distances create regulatory networks that control gene expression and differentiation (de Wit and de Laat, 2012; Liu et al., 2011; Montavon et al., 2011).

Irreversible developmental decisions, such as those made by differentiating neurons, employ diverse epigenetic mechanisms to lock in transcriptional status for the life of a cell. Placing genes in subnuclear compartments compatible or incompatible with transcription could finalize these decisions. The differentiation of olfactory sensory neurons (OSNs) provides an extreme example of such developmental commitment; OSNs choose one out of ~2,800 olfactory receptor (OR) alleles and subsequently establish a stable transcription program that assures that axons from like neurons converge to distinct glomeruli (Buck and Axel, 1991; Imai et al., 2010). The monoallelic nature of OR expression (Chess et al., 1994), together with the observation that OR promoters are extremely homogeneous and share common regulatory elements (Clowney et al., 2011), implies that DNA sequence is not sufficient to instruct the expression of only one allele in each neuron and that an epigenetic mechanism is in place. Indeed, the discovery of OR heterochromatinization argues for epigenetic, nondeterministic control of OR choice (Magklara et al., 2011). Because active OR alleles have different chromatin modifications from the inactive ORs (Magklara et al., 2011) and associate in *cis* and *trans* with the H enhancer (Lomvardas et al., 2006), this epigenetic regulation might have a spatial component. Although deletion of H does not have detectable effects on the transcription of most ORs (Khan et al., 2011), its association with active OR alleles could reflect the physical separation of the active OR allele from silent OR genes and its transfer to an activating nuclear factory.

Here, we examine the significance of nuclear organization in OR expression. Using a complex DNA FISH probe that recognizes most OR loci, we demonstrate OSN-specific and

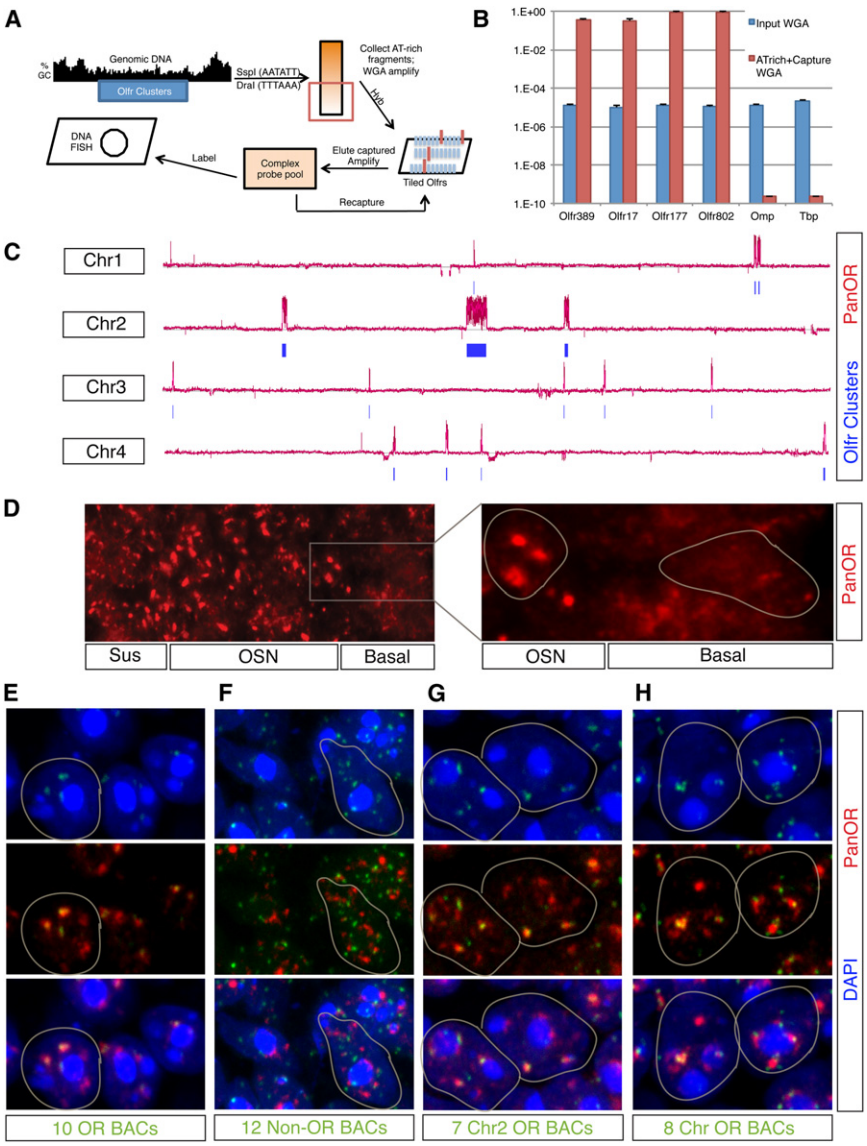

Figure 1. Visualizing the Nuclear Distribution of OR Loci

(A) Schematic of sequence-capture-based DNA FISH probe construction.

(B) qPCR analysis of panOR library showing enrichment for four different ORs, but not for control genes. Error bars display SEM between duplicate PCR wells.

(C) Microarray analysis of panOR probe. Blue bars represent the chromosomal location of OR clusters, and red represent hybridization signal intensity produced by MA2C analysis using a sliding window of 10 Kb, with minimum number of probes 20 and maximum gap of probes 1 Kb.

(D) Wide-field image of DNA FISH on MOE sections with panOR probe. OR foci are detected only in OSNs. In sustentacular cells (apical layer on the left) and basal cells (basal layer on the right), the DNA FISH signal is diffuse. In the zoomed-in view on the right, we highlight the nuclear borders of a basal cell and a neuron.

(E–H) DNA FISH on MOE sections with panOR probe (red) and BAC probe pools (green). OR BACs (E) colocalize with panOR, whereas non-OR BACs (F) do not. Pooled OR BACs across chromosome 2 (G) coalesce into optically indiscrete signals in OSNs. Pooled OR BACs covering clusters on eight separate chromosomes (H) (Chr1, 2, 3, 7, 9, 14, 15, and 16) occupy the same panOR focus. Maximum intensity Z projections of three micron confocal stacks are shown. Borders are drawn around nuclear edges.

See also Figure S1 and Tables S1, S2, and S4.

differentiation-dependent intra- and interchromosomal aggregation of silent ORs. Whereas these OR-specific foci colocalize with H3K9me3, H4K20me3, and heterochromatin protein 1 β (HP1β), the active OR alleles have minimal overlap with heterochromatic markers and reside in euchromatic territories, suggesting the existence of repressive and activating nuclear compartments for OR alleles. Critical for this nuclear organization is the downregulation and removal of lamin b receptor (LBR) from the nuclear envelope of OSNs. Deletion of LBR causes ectopic aggregation of OR loci in basal and sustentacular cells in the main olfactory epithelium (MOE), whereas expression of LBR in OSNs disrupts the formation of OR foci, resulting in decompaction of OR heterochromatin, coexpression of a large number of ORs, overall reduction of OR transcription, and disruption of OSN targeting. Our analysis provides evidence for an instructive role of nuclear architecture in monogenic olfactory receptor expression.

RESULTS

ORs and other AT-rich gene families frequently associate with the nuclear lamina (Peric-Hupkes et al., 2010). However, our DNA FISH analysis with individual BAC probes failed to reveal a significant distribution of OR loci toward the nuclear periphery of OSNs (Lomvardas et al., 2006). To obtain a comprehensive view of the distribution of OR loci in OSN nuclei, we sought to generate a DNA FISH probe that would allow the simultaneous detection of most OR loci. First, because OR clusters reside in extremely AT-rich isochores (Clowney et al., 2011; Glusman et al., 2001), we digested genomic DNA with restriction enzymes that recognize AT-rich sequences and collected DNA fractions with significant enrichment for ORs. Next, these were amplified and subjected to a second round of purification by sequence capture on a custom tiling array covering OR clusters (Figure 1A) (Albert et al., 2007). This high-density array contains oligonucleotides against the unique sequences within the 46 OR genomic clusters, spanning a total region of 40 MB. Two rounds of capture, elution, and amplification produced a DNA library highly enriched for OR sequences. Quantitative PCR analysis (qPCR) of the final amplicon detects only sequences from OR clusters, suggesting the elimination of unique, non-OR DNA (Figure 1B).

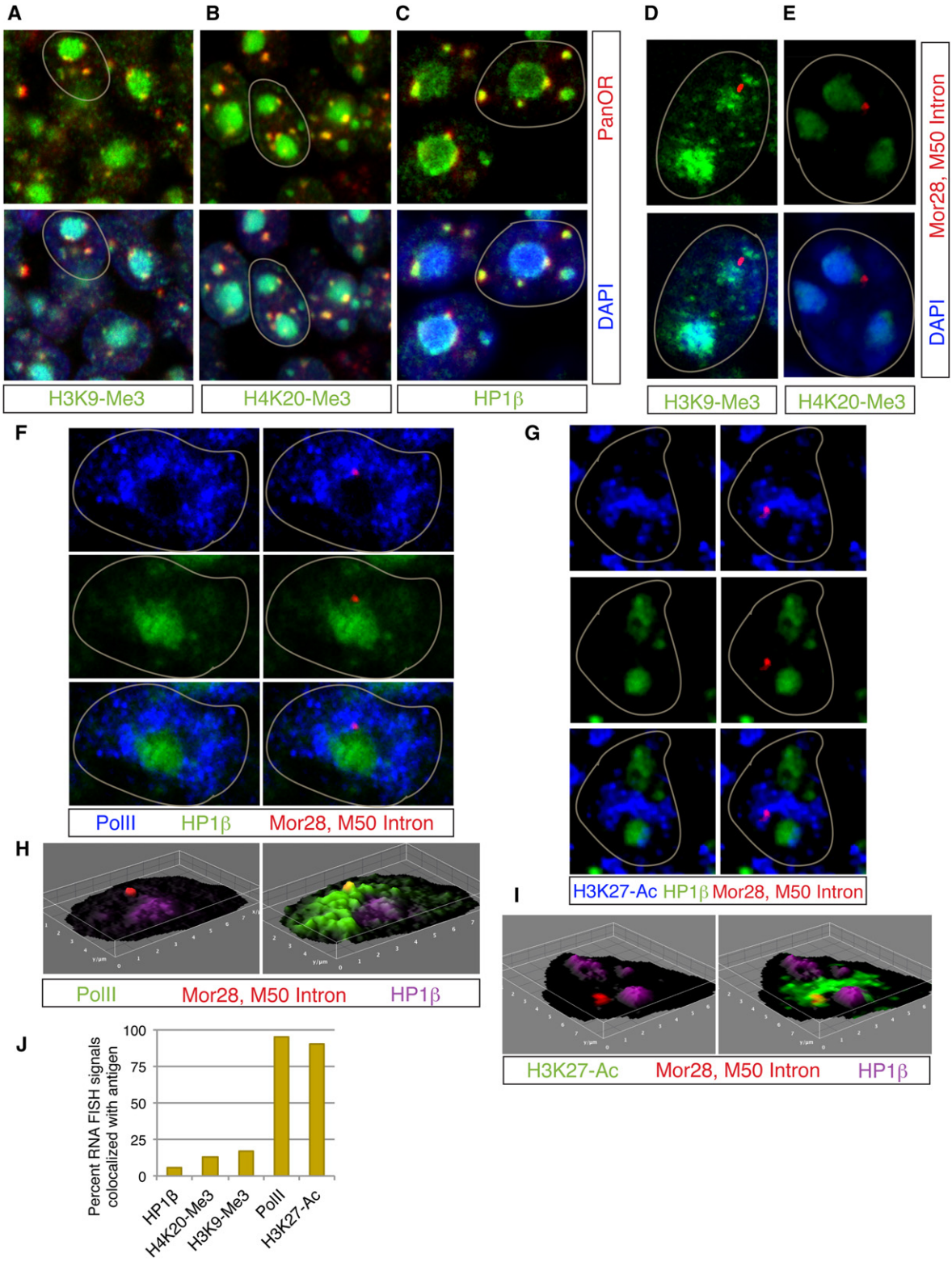

Figure 2. OR Foci Are Heterochromatic Aggregates from which the Active Allele Escapes

(A–C) IF for H3K9me3 (A), H4K20me3 (B), or HP1β (C) (green) combined with panOR DNA FISH (red) in MOE sections.

(D–G) Nascent RNA FISH using pooled introns of ORs MOR28 and M50 (red) combined with IF against H3K9me3 (D, green), H4K20me3 (E, green), HP1β (F and G, green), RNA polymerase II (F, blue), and H3K27-Acetyl (G, blue).

To further examine the composition of this DNA library, we analyzed its contents by whole-genome microarray hybridization, using a tiling array covering mouse chromosomes 1 to 4. This analysis demonstrates the sensitivity and selectivity of our purification strategy: the probe detects 340 of 346 OR genes located on these 4 chromosomes, 40 of ~80 non-OR genes located *cis* to OR clusters (and included on the capturing array), and 6 of ~5,000 non-OR genes (FDR < 0.05, 98.2% sensitivity, 98.4% OR cluster specificity, $p \leq 10^{-72}$) (Figures 1C and Figures S1B–S1D and Table S1 available online).

OSN-Specific Aggregation of OR Genes

We used this "panOR" library as a probe for DNA FISH experiments on sections of the MOE. Although there are 92 OR clusters in the diploid nucleus, the panOR probe detects an average of ~5 large foci in OSNs (Figure 1D). This unexpected distribution is specific for OSNs: OR distribution in other cell populations represented in MOE sections (undifferentiated basal cells and sustentacular cells) is diffuse and more consistent with a random arrangement of the 92 OR clusters or ~2,800 alleles. Quantification of the distribution of the DNA FISH signal in the three cell types of the MOE across the same sections in the same experiments supports this conclusion (Figure S1E–S1F): high-intensity pixels (above 120 in the 8 bit range of 0–255) were found only in OSNs and not in sustentacular or basal cells. To quantify the distribution of panOR signal, we calculated standard deviation of signal intensity across nuclear space. Average standard deviation in OSNs is 42.3, indicating spotty signal distribution, and is 9.3 or 11.3 in basal and sustentacular cells, indicating smoother distribution (n > 100 for each cell type). Finally, DNA FISH with this probe in other neuronal types demonstrates a diffuse distribution of OR loci (data not shown and Figure S2D), arguing for an OSN-specific nuclear pattern.

The focal nature of the panOR DNA FISH signal suggests that OR alleles from different OR clusters merge in distinct nuclear regions during OSN differentiation. To test this, we pooled 10 OR- or 12 non-OR-BAC probes and performed two-color DNA FISH with the panOR probe. There was extensive colocalization between the panOR probe and OR BAC probes (Pearson's coefficient r = 0.637, Mander's coefficient of BAC signal colocalizing with panOR M1 = 0.835, n > 100) and little colocalization between the panOR probe and the non-OR BACs (r = 0.187, M1 = 0.109, n > 100) (Figures 1E and 1F and Table S2), suggesting selectivity for OR loci in the composition of these aggregates (Figure S1I). Though the panOR probe includes most OR loci, lack of complete overlap between the panOR and the individual OR BAC probes was expected. The panOR probe is 200-fold more complex than each BAC, and it is outcompeted for binding at ORs targeted by a BAC. Thus, BAC signals colocalized with panOR signal represent OR alleles surrounded by other OR loci labeled by the panOR probe at distances below the optical resolution of confocal microscopy.

The combined OR BACs produce fewer DNA FISH spots in the OSNs (3.94 spots/nucleus/Z stack, n = 38) than in sustentacular (9.1 spots, n = 38) or basal cells (8.52 spots, n = 30), providing an independent verification for the extensive aggregation of these loci: they are optically indiscrete significantly more often in OSNs than in basal and sustentacular cells. Non-OR BAC probes did not appear more aggregated in the OSNs (10.08 spots in OSNs, 6.4 in sustentacular, and 7.1 in basal cells, n = 30 for each cell type).

To explore the contribution of intra- and interchromosomal interactions to the formation of OR foci and the colocalization of ORs, we used two additional pools of OR BACs, one containing seven BACs targeting three clusters on chromosome 2 and the other containing eight BACs, each targeting a cluster from a different chromosome. These pools, when combined with panOR probe, revealed two layers of organization in OSNs: alleles within the same cluster coalesce into optically indiscrete signals, whereas clusters from different chromosomes generate distinguishable signals inside the same panOR focus (Figures 1G and 1H). The BACs from the same chromosome produce 5.9 dots in sustentacular cells and 2.3 dots in OSNs (n = 30 for each), whereas BACs from different chromosomes produce equal numbers of dots in both cell types. However, multiple OR BAC dots from different chromosomes were seen in 50% of the panOR foci, and more than two dots per aggregate in 29% of the cells (n = 50) (Figure 1H). Moreover, maternal and paternal alleles of the same OR cluster reside in the same OR aggregate in ~6% of the tested OSNs (Figure S1H). Finally, panOR foci do not colocalize with large repeat classes, pericentromeric heterochromatin (PH), or other multigene families (Figures S2A–S2C and data not shown), suggesting that the aggregation of OR clusters produces distinct and selective OR gene territories.

Spatial Segregation between Active and Silent OR Alleles

To reveal the epigenetic signature of OR foci, we combined DNA FISH analysis with immunofluorescence (IF) against the heterochromatic marks found on ORs (Magklara et al., 2011) or heterochromatin-binding protein 1 β (HP1β), the only heterochromatic HP1 member expressed in OSNs (data not shown). This analysis reveals overlap between the OR foci, H3K9me3, H4K20me3, and HP1β (Figures 2A–2C and Table S2), but not with Pol II (Figure S2E), consistent with a heterochromatic nature of these aggregates. This colocalization is differentiation dependent and cell type specific; we do not detect overlap between the two signals in basal cells in the MOE or in retinal neurons (Figure S2D).

We then performed nascent RNA FISH on sections of the MOE using intronic probes against OR genes MOR28, M50, M71, and P2 combined with IF for H3K9me3, H4K20me3, or HP1β. In contrast with the bulk of the panOR signal, active OR alleles

(H and I) 3D surface color plots corresponding to cells from (F) and (G), respectively. The luminance of the image is interpreted as height for the plot. Nascent OR transcript is shown in red, HP1β in magenta, and Pol II (H) or H3K27 acetyl (I) in green.

(J) Manual colocalization counts for nascent transcript and antigens as presented in (D–G). Signals were counted as colocalized when there was some overlap between nascent transcript and antigen. n = 150 for HP1β, 31 for H4K20me3, 12 for H3K9me3, 64 for Pol II, and 64 for H3K27-Ac.

See also Figure S2 and Table S2.

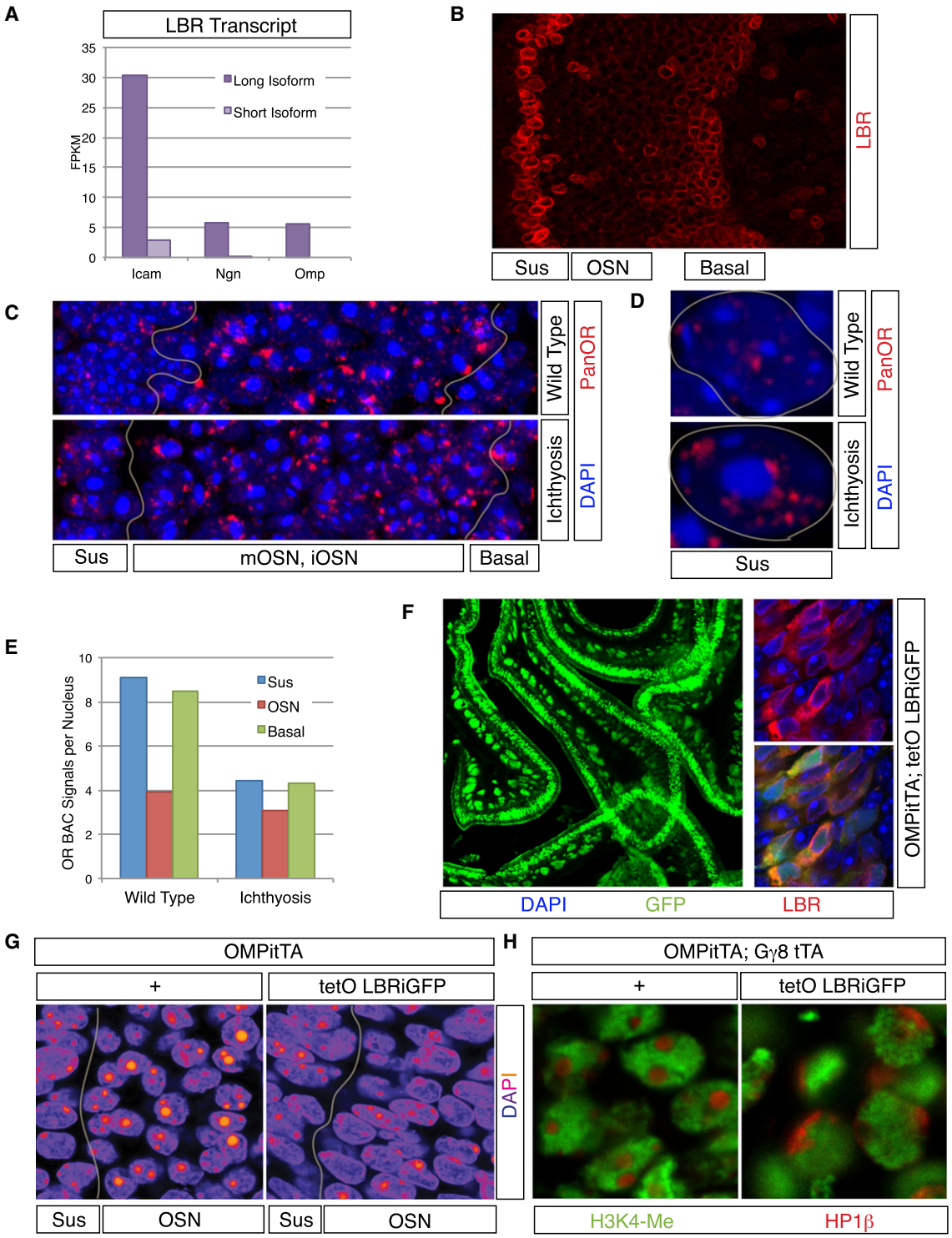

Figure 3. LBR Regulates Nuclear Topology in the MOE

(A) LBR transcript levels determined by RNA-seq analysis on FAC-sorted populations from the MOE. LBR decreases from horizontal basal cells (ICAM+) to intermediate progenitors (Ngn+) to mature OSNs (OMP+).

(B) IF against LBR in the MOE. Sustentacular and basal cells contain LBR in their nuclear envelopes, whereas OSNs do not. Occasional LBR+ cells in the neuron layer are migrating nonneuronal cells.

(C and D) PanOR DNA FISH (red) in MOE sections of Ichthyotic or control animals shown in low magnification (C). Sustentacular and basal cells have PH cores and panOR foci in Ichthyotic animals. (D) High-magnification image of a control and an Ichthyotic sustentacular cell.

have little overlap with any of the three heterochromatic marks (Figures 2D–2J, S2F, and S2G and Table S2). We also combined nascent RNA FISH with IF for Pol II or H3K27-Acetyl and H4K20me3 or HP1β (Figures 2F–2J and Table S2). These experiments corroborate that the active OR allele is spatially segregated from the silent ORs and resides in euchromatic territory.

LBR Organizes the Topology of OSN Nuclei

It is intriguing that most OR genes and PH are located near the center of OSN nuclei instead of being distributed toward the nuclear envelope (Figure S1A). This "inside-out" nuclear morphology is reminiscent of the nuclear architecture reported in homozygous Ichthyosis mice, a spontaneous LBR loss-of-function mutant (Goldowitz and Mullen, 1982). LBR is a nuclear envelope protein that interacts with HP1 and heterochromatin (Hoffmann et al., 2002; Okada et al., 2005; Pyrpasopoulou et al., 1996). RNA-seq revealed a continuous reduction in LBR mRNA levels during differentiation from HBCs to OSNs, and IF confirmed that whereas LBR is present in the nuclear envelope of basal and sustentacular cells, it is absent in the neuronal lineage of the MOE (Figures 3A, 3B, and S3A).

PanOR DNA FISH on MOE sections from the Ichthyosis mice revealed no changes in OR aggregation in OSNs, which already lack LBR. However, nuclear architecture and OR organization of Ichthyotic basal and sustentacular cells approach that of wild-type OSNs (Figures 3C, 3D, and S3B). PH forms large, centrally located foci in both cell types, and ORs form aggregates at the periphery of the pericentromeric foci. According to the pooled BAC assay in the Ichthyosis mouse, the number of DNA FISH spots is uniform among the three cell types, and the basal and sustentacular cells have similar numbers of DNA FISH spots to control OSNs (Figure 3E), supporting a role for LBR downregulation in OR aggregation. Because ectopic OR aggregation occurs in two cell types that do not express ORs and likely do not contain the transcription factors responsible for OR activation, an effect of this mutation on OR expression and OSN targeting is unlikely and was not detected (data not shown and Figure S3C).

Thus, we sought to perform the opposite experiment: to restore LBR expression to OSNs instead of removing LBR from cells that do not express ORs. We generated a tetO LBR-IRES-GFP transgenic mouse that we crossed to OMP-IRES-tTA mice to achieve expression of LBR in OSNs. One transgenic line expresses the transgene in a significant proportion of OSNs (Figure 3F). Like endogenous LBR, transgenic LBR is restricted to the nuclear envelope without diffusing in the nucleoplasm (Figure 3F).

We used this transgenic line to analyze the effects of ectopic LBR expression on the nuclear morphology of mOSNs. DAPI staining becomes less intense, and PH is moved toward the nuclear periphery of LBR+ OSNs (Figures 3G and S3D). OSNs in these sections that do not express the transgene have morphology similar to wild-type nuclei (Figure S3D). IF shows HP1β recruitment to the nuclear envelope in LBR+ OSNs, whereas centrally shifted euchromatin occupies most of the nucleus (Figures 3H, S3E, and S3F). Thus, ectopic LBR expression in a postmitotic cell is sufficient to reverse the "inside-out" arrangement and to recruit PH to the nuclear periphery.

Ectopic LBR Expression Decondenses OSN Heterochromatin

IF does not provide information about the structural and biophysical changes occurring in OSN chromatin upon ectopic LBR expression. To obtain this information, we imaged control and LBR+ OSNs with soft X-ray tomography (SXT), a high-resolution imaging method that is applied to fully hydrated, unfixed, and unstained cells and measures carbon and nitrogen concentration in biological samples (McDermott et al., 2009). Orthoslices (computer-generated sections) and three-dimensional (3D) reconstructions of SXT imaging of control OSNs reveal that the more condensed (darker) chromatin is located at the center of the nucleus, in agreement with the morphology seen by IF (Figures 4A, 4B, and 4G and Movie S1). We also detect extremely condensed structures at the periphery of this PH core that are specific for this cell type; only sperm nuclei have chromatin particles with higher compaction values (data not shown). Although the arrangement of these dark foci is similar to the arrangement of the OR foci around the PH core of the OSN nucleus, DNA FISH or IF are incompatible with SXT, and therefore it is impossible to prove directly that these are the same structures.

SXT imaging of LBR+ OSNs shows the relocation of the most condensed chromatin toward the nuclear membrane (Figures 4D, 4E, and 4H and Movie S2). Moreover, LBR expression increases the nuclear volume from $105u^3$ to $135u^3$ and induces the folding of the nuclear membrane and an overall change in the nuclear shape (Figures 4C and 4F and Movies S3 and S4). Overall, chromatin decondensation induced by LBR expression in OSNs is quantitatively described by measurements of the linear absorption coefficient (LAC) (McDermott et al., 2009) of control and LBR+ OSNs (Figure 4I). This measurement, which depicts the concentration of organic material per voxel, corroborates the loss of the densest foci upon LBR expression. Thus, if condensed regions correspond to OR foci, ectopic LBR expression should cause decompaction of OR heterochromatin. DNaseI sensitivity experiments (Magklara et al., 2011) in nuclei from fluorescence-activated cell-sorted (FAC-sorted) control or LBR+ OSNs confirms a significant decompaction of OR and pericentromeric heterochromatin upon LBR expression (Figure 4J).

(E) Quantification of number of optically discrete foci formed by a pool of OR BAC probes (as in Figure 1E) in sustentacular, OSN, and basal cell types in control and Ichthyotic MOE sections. $n \geq 30$ for all groups. $p < 0.0001$ for comparison between OSN and sustentacular or basal cells in control animals and for comparison across sustentacular or across basal cells in control versus Ichthyosis tissue (Student's t test).
(F) GFP expression and LBR IF in MOE sections from a tetO LBR-IRES-GFP; OMP-IRES-tTA mouse. Low-magnification image at left shows GFP signal across the OE; high-magnification image at right shows that GFP (green) and LBR (red) are coexpressed and transgenic LBR is restricted to the nuclear envelope.
(G) False-color image of DAPI staining in LBR-expressing OSNs versus control OSNs shows loss of OSN-specific PH core (gold) upon LBR expression.
(H) IF in control and LBR+ animals for H3K4-Me1 and HP1β shows reorganization of the OSN nucleus upon LBR expression.
See also Figure S3.

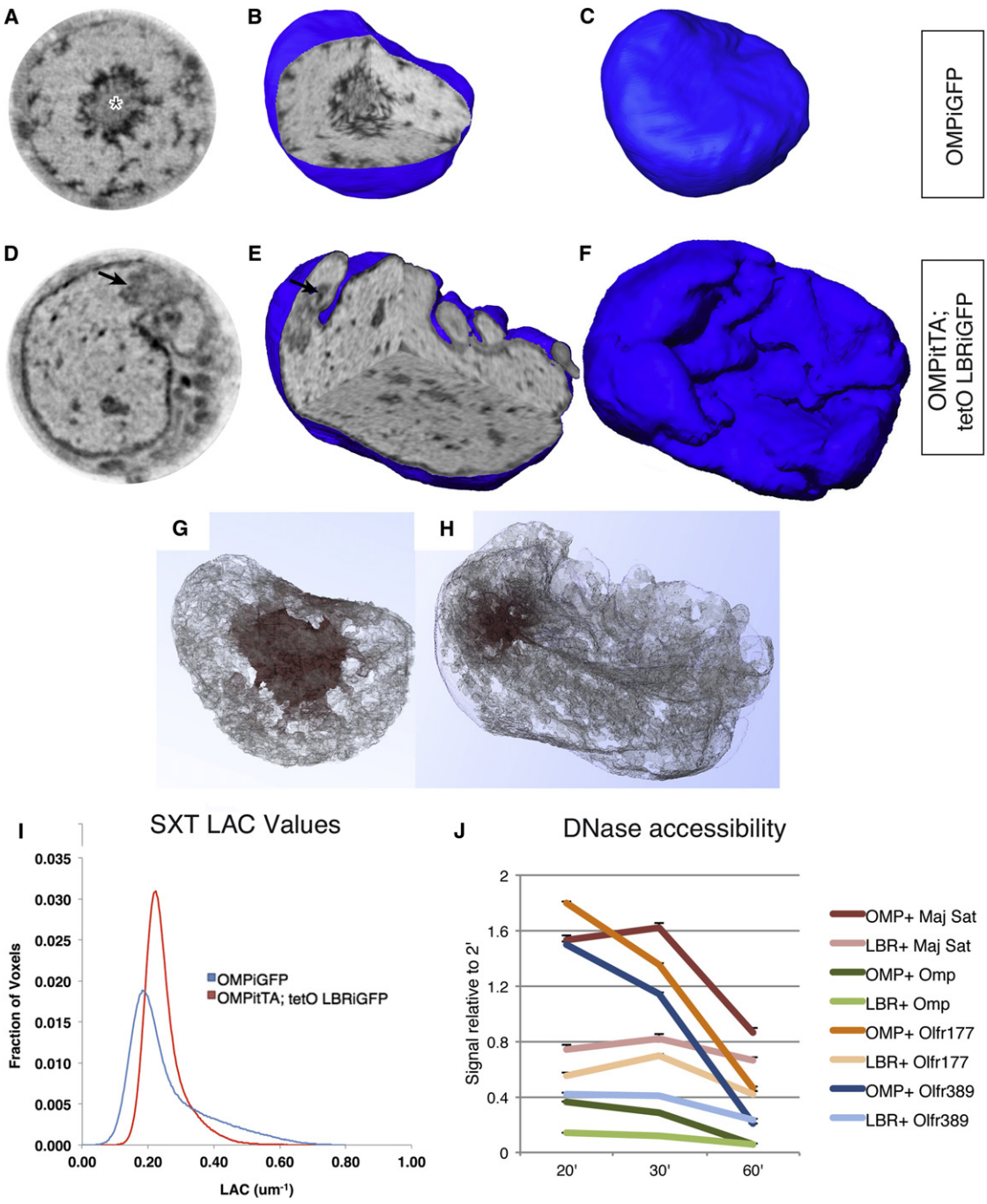

Figure 4. Soft X-Ray Tomography of OSNs Demonstrates Chromatin Decompaction and Nuclear Reorganization upon LBR Expression

(A) An orthoslice from the tomographic reconstruction of a GFP+ neuron from an OMP-IRES-GFP mouse. PH (asterisk) surrounded by condensed, OSN-specific foci can be seen in the center of the nucleus; only small amounts of heterochromatin are tethered to the nuclear envelope.

(B and C) Segmented nucleus (blue; obtained by manually tracing the nuclear envelope through all orthoslices of the reconstruction) seen in a 3D cutaway view with three orthogonal orthoslices (B) shows that the pericentromeric heterochromatin is in the center of the nucleus and the nuclear envelope is not folded (C).

(D) Orthoslice from an OMP-IRES-tTA; tetO LBR-IRES-GFP mouse. The dark particles that surround the PH core in the control OSN nucleus are not present in LBR-expressing nucleus. PH (arrow) is positioned just beneath the highly folded nuclear envelope upon LBR expression. The nuclear envelope is thicker, likely due to the presence of LBR and the recruitment of heterochromatin.

(E and F) Three-dimensional cutaway view showing the increased nuclear volume (E) and marked folding of the nuclear envelope, which is more apparent in the surface view (F).

(G) Still frame of Movie S1 from the control OSN shown in (A). The nucleus was segmented from the tomographic reconstruction using the 3D linear absorption coefficient (LAC). It is shown here using a transparent surface view to reveal the chromatin. To aid visualization, the opacity and color of the obtained surface were

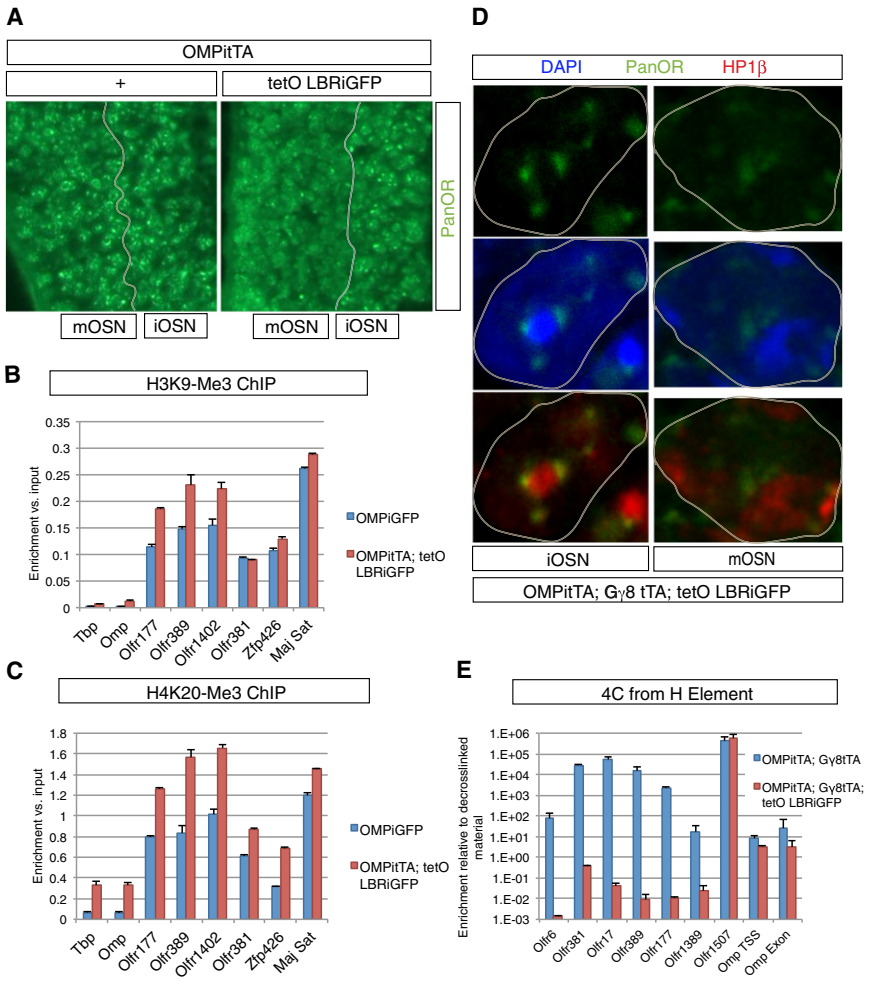

Figure 5. LBR Expression Disrupts OR Foci

(A) Wide-field image of panOR DNA FISH (green) in MOE sections from control (left) and LBR-expressing transgenic mice (right). Line depicts the borders between immature and mature OSNs. Transgenic LBR expression driven by OMP-IRES-tTA is restricted to the mature OSNs, where OR foci are disrupted.

(B and C) ChIP-qPCR analysis of H3K9me3 (B) and H4K20me3 (C) enrichment in FAC-sorted control (OMP-IRES-GFP, blue bars) or LBR-expressing (OMP-IRES-tTA; tetO LBR-IRES-GFP, red bars) OSNs. Error bars display SEM between duplicate PCR wells. Similar results were obtained from biological replicates.

(D) IF for HP1β (red) combined with panOR DNA FISH (green) in MOE sections from LBR-expressing transgenic mice. The panels on the left depict an immature neuron that has not expressed the transgene yet, whereas the panels on the right show an LBR+ OSN from the same section. OR loci lose their association with HP1β upon LBR expression.

(E) qPCR analysis comparing the enrichment of OR sequences in a 4C library constructed by inverse PCR from the H enhancer from wild-type and LBR-expressing MOEs. Enrichment values were normalized to control material decrosslinked before ligation. Error bars display SEM between duplicate PCR wells.

See also Figure S4 and Table S2.

Ectopic LBR Expression Disrupts OR Aggregation

The spatial reorganization of HP1β, the elimination of the dark foci detected by SXT, and the increase in DNase sensitivity of OR chromatin suggest that ectopic LBR expression disrupts the aggregation of OR loci. To test this, we performed DNA FISH with the panOR probe in sections of LBR-expressing transgenic mice. Low-magnification images show significant effects of ectopic LBR expression on the distribution of OR loci. In the apical LBR+ neuronal layer, the intense OR foci dissolve; in contrast, immature OSNs and progenitors that do not yet express the transgene but have already downregulated the endogenous LBR retain a focal OR arrangement (Figures 5A and S4A).

To investigate whether altering the tertiary organization of OR loci affects the epigenetic characteristics of these genes, we examined association of OR genes with H3K9me3, H4K20me3, and HP1β in LBR+ OSNs. H3K9me3 and H4K20me3 remained enriched on OR loci upon LBR expression by native ChIP-qPCR assays on FAC-sorted OSNs (Figures 5B and 5C) and FISH-IF (Figures S4B and S4C and Table S2). In contrast, association of OR loci with HP1β was reduced as measured by FISH-IF (Figures 5D and Table S2). Reduction in

mapped to a 3D color field with the same dimensions as the whole-cell data set. The color field and color map were chosen to highlight the condensed chromatin in the center of the nucleus so that the most condensed chromatin is dense brown with low transparency and the remaining chromatin is gray with a high degree of transparency.

(H) Still frame of Movie S2 from the LBR+ OSN shown in (D). The nucleus was segmented as in (D), and the color coding depicts the same LAC values. The color field and color map highlight the acentric, condensed chromatin abutting the nuclear envelope. There is also a notable reduction in the volume of condensed chromatin (brown) and complete loss of the most condensed OSN-specific foci.

(I) Histogram of linear absorption coefficients of each voxel in control and LBR-expressing mOSNs. Dense voxels (LAC > 0.4 um^{-1}) that are OSN specific and depict the most compacted chromatin are lost in LBR-expressing nuclei.

(J) qPCR analysis of DNase digestion time course assay in sorted control OMP+ (OMP-IRES-GFP) or LBR+ (OMP-IRES-tTA; tetO LBR-IRES-GFP) olfactory neurons. OR (orange, blue) and satellite (red) loci that are heterochromatinized and DNase resistant in control OSNs are DNase sensitive in LBR+ OSNs. Control euchromatic sequence (Omp, green) is DNase sensitive in both cell types. Pale shades denote LBR+ cells, and dark shades denote control cells. Error bars display SEM between duplicate PCR wells. Similar results were obtained from biological replicates.

See also Movies S1,S2,S3,S4.

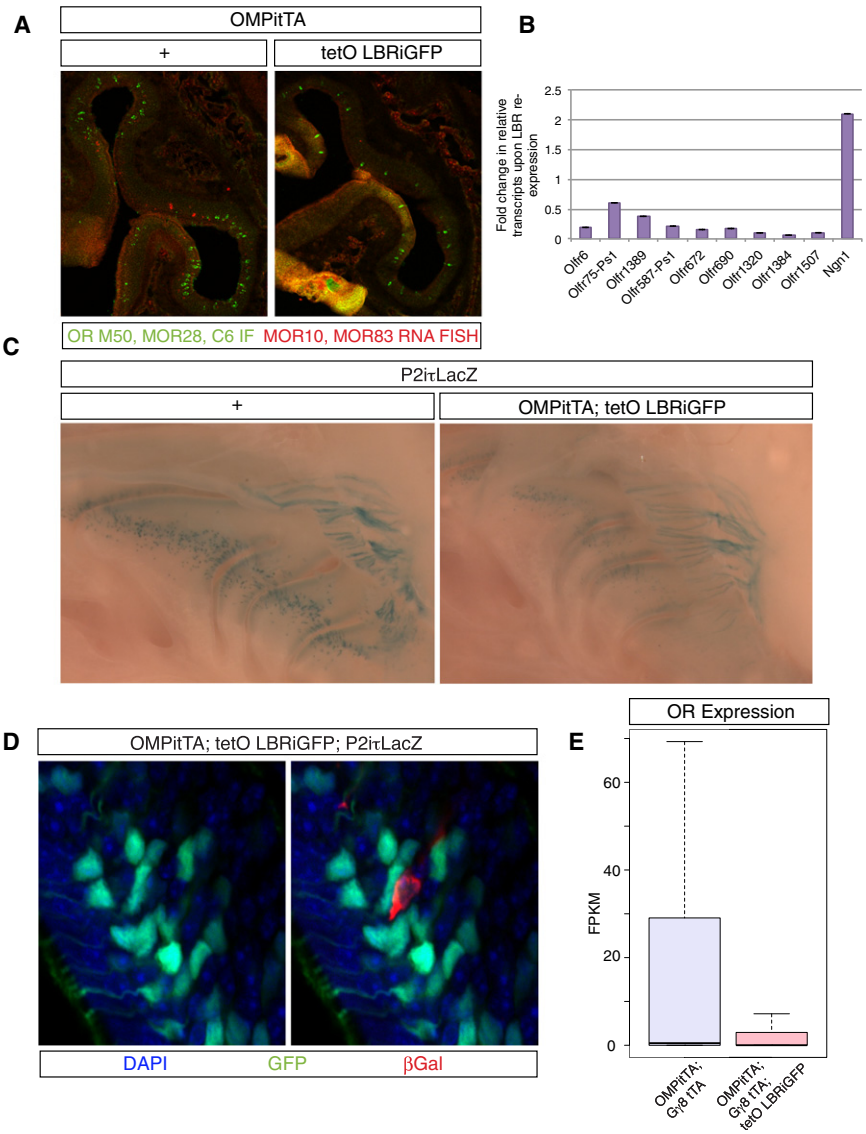

Figure 6. LBR Expression Inhibits OR Transcription

(A) RNA FISH and IF against pools of ORs in MOE sections from control or LBR-expressing transgenic mice.

(B) qRT-PCR in FAC-sorted GFP$^+$ OSNs from OMP-IRES-GFP or OMP-IRES-tTA; tetoLBR-IRES-GFP mice. qRT-PCR values from each cell population were normalized to actin (which is not affected by LBR expression), and the results are shown as fold difference (LBR-expressing OSNs/control OSNs). Error bars display SEM between duplicate PCR wells, and similar results were obtained from biological replicates.

(C) Whole-mount X-gal staining of MOEs from control or LBR-expressing P2-IRES-τLacZ mice.

(D) IF for β-gal and GFP in MOE sections from LBR-expressing P2-IRES-τLacZ mice. β-gal positive neurons do not express the transgenic LBR, as shown by the absence of GFP signal.

(E) RNA-seq analysis of ORs in control versus LBR-expressing MOEs.

See also Figure S5.

overlap between H4K20me3 and HP1β was also observed in the LBR+ OSNs. Thus, despite retaining heterochromatic histone marks, OR loci lose their aggregated arrangement and their nonhistone heterochromatic coat upon LBR expression, which is consistent with the increased DNase sensitivity.

In wild-type OSNs, active OR alleles interact with the H enhancer. To test whether LBR expression also abrogates interchromosomal interactions between the active allele and H, we performed circularized chromosome conformation capture (4C) using inverse H PCR primers as previously described (Lomvardas et al., 2006) on LBR-expressing or control MOEs. To increase the proportion of LBR-expressing cells in this mixed population, we combined two tTA drivers (OMP-IRES-tTA and Gγ8 tTA). The enrichment of various OR sequences in this 4C library was assayed by qPCR. LBR expression in OSNs results in the loss of most H-OR associations. In LBR transgenics, H retains only its interaction with the linked OR MOR28 (*Olfr1507*) located 75 Kb downstream (Figure 5E). Therefore, ectopic LBR expression in OSNs not only prevents heterochromatic OR aggregation, but also disrupts the interaction between the H enhancer and unlinked ORs.

LBR Expression Inhibits OR Transcription

IF and RNA FISH experiments in MOE sections from control and LBR-expressing mice revealed a 3-fold reduction in the numbers of neurons expressing particular ORs in the transgenic mice (Figure 6A). Importantly, most neurons that retain high-level OR expression do not express transgenic LBR (data not shown and Figure 6D). For more quantitative measure of the effects of LBR in OR expression, we used FAC-sorting to isolate control or LBR+ OSNs and performed quantitative, reverse-transcriptase PCR (qRT-PCR). This analysis supports that LBR expression has significant inhibitory effects on OR expression (Figure 6B). Similarly, whole-mount X-gal staining in MOEs from P2-IRES-τLacZ mice crossed to LBR-expressing transgenics shows reduced X-gal signal, supporting a repressive effect on OR expression (Figure 6C). Neurons that retained high β-gal protein expression often failed to express the LBR transgene, as demonstrated by IF for β-gal and GFP in sections of these mice (Figure 6D). Because OMP drives LBR expression only after OR choice, this result indicates postchoice downregulation of this P2 allele and the rest of the OR repertoire.

To test whether the inhibitory effects of LBR expression apply to genes that do not follow the spatial regulation of endogenous OR genes, we used a transgenic OR that is under the control of the tetO promoter (tetO MOR28-IRES-τLacZ). This transgene

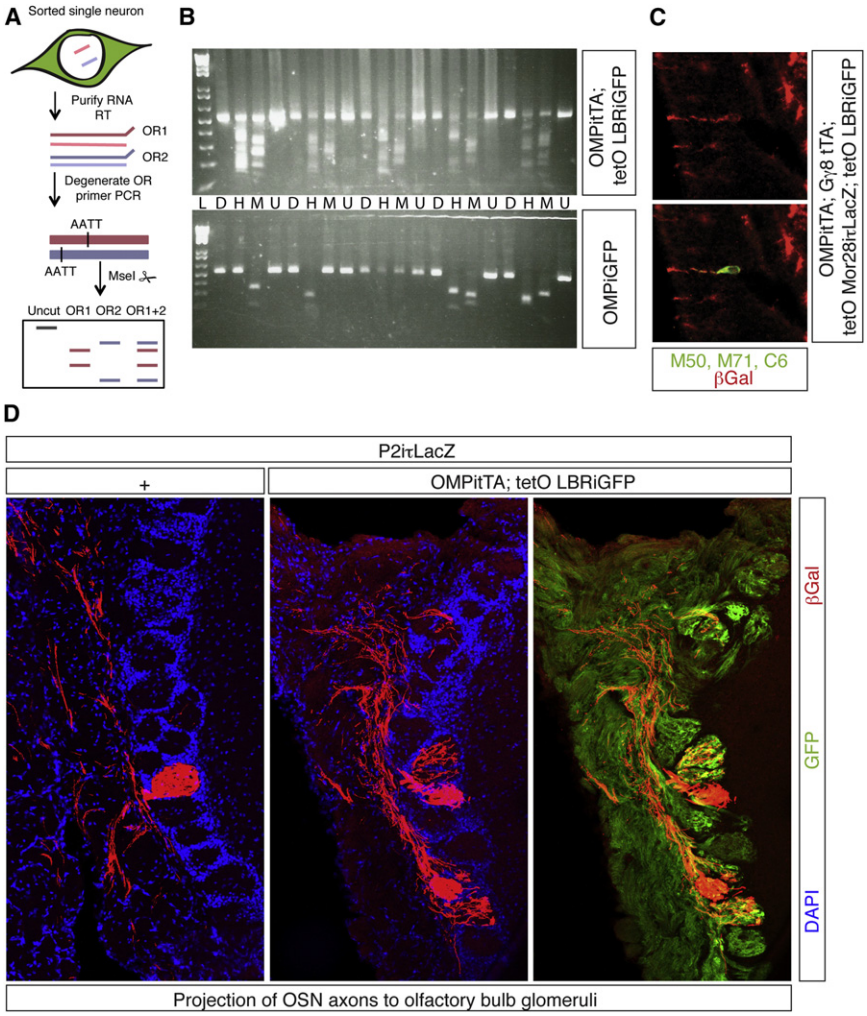

Figure 7. LBR Expression Induces OR Co-expression and Ectopic Targeting to the Olfactory Bulb

(A) Schematic of single-cell degenerate OR digest.

(B) Agarose gel electrophoresis of degenerate OR PCR amplicons from single-cell cDNA libraries prepared from sorted control (OMP-IRES-GFP) or LBR-overexpressing (OMP-IRES-tTA; tetoLBR-IRES-GFP) OSNs. Amplicons digested with DraI (marked with D), HinfI (marked with H), MseI (marked with M), or undigested (marked with U) from five control and five LBR+ cells are shown.

(C) IF for β-gal (red) and ORs M50, M71, and C6 (green) in MOE sections from OMP-IRES-tTA; Gγ8 tTA; tetOLBR-IRES-GFP; tetOMOR28-IRES-LacZ mice. Two percent of the neurons expressing one of the three endogenous ORs ($n > 1,000$) are β-gal positive.

(D) IF for β-gal (red) in sections of the olfactory bulb of control and LBR-expressing P2-IRES-τLacZ mice. Medial P2 glomerular region is shown. Axons from the LBR-expressing neurons are also GFP positive (green). Nuclei are counterstained with DAPI.

See also Figure S6 and Table S3.

also carries H3K9me3 and H4K20me3 (data not shown), but unlike the endogenous ORs, its heterochromatization is not OSN specific and is probably caused by its multicopy (16 tandem copies) insertion (Garrick et al., 1998). This transgene does not interact with either the endogenous ORs or the H enhancer (Figure S1I and data not shown). In agreement with the repressive signature of this transgene, its expression is sporadic when crossed to the OMP-IRES-tTA driver but increases in frequency when crossed to LBR-expressing transgenics (Figure S5B). This is consistent with a simple mode of gene regulation in which chromatin decompaction allows tTA binding on the tetO promoter in more cells and transcriptional activation at higher frequency; such a linear and straightforward model does not apply to the endogenous ORs.

To determine the genome-wide effects of LBR expression in OSNs, we performed RNA-seq from whole MOE preparations. To increase the proportion of LBR+ OSNs in this mixed population, we combined two tTA drivers (OMP-IRES-tTA and Gγ8 tTA). In agreement with the observations in the FAC-sorted neurons, LBR expression in OSNs induces an ~8-fold downregulation of total OR expression (Figure 6E). Though OR expression is downregulated, most of the genes detected in OSNs (~14,000 genes) are not affected by ectopic LBR expression (367 non-OR transcripts significantly downregulated and 873 transcripts significantly upregulated, Cuffdiff FDR 0.05, genes with at least 10 reads). Interestingly, expression of some markers of immature OSN and progenitor cell populations increases in these animals (Figure S5A). Overall, these changes suggest a partial transition toward a less-differentiated state, rather than elimination of mature OSNs, as shown by the lack of increased apoptosis in the transgenic MOE (Figure S5C).

Ectopic LBR Expression Disrupts the Singularity of OR Transcription

Downregulation of OR transcription in LBR+ neurons is counterintuitive considering that the accessibility of OR chromatin increases and that these loci are stripped from HP1β. The disruption of long-range interactions with activating enhancers, like H, could contribute to this downregulation. Moreover, although global decompaction of OR chromatin might make all of the OR alleles transcriptionally competent, it is possible that OSNs cannot support transcription of ~2,800 OR alleles at the levels of a singularly transcribed OR. To test this, we performed single-cell RT-PCR with degenerate OR primers, followed by restriction enzyme digestion and electrophoresis (Buck and Axel, 1991; Figures 7A and S6A). We obtained 10 single-cell cDNA libraries from each genotype (see Extended Experimental Procedures) and examined OR representation by DraI, HinfI, and MseI digestion.

The complexity of the degenerate OR amplicons is different between control and LBR+ OSNs. In every LBR+ OSN, the base pair sum of the individual digestion products exceeds the length of the undigested PCR, whereas control amplicons contain only one product (Figure 7B, showing five amplicons from each genotype. Similar results were obtained for the other five amplicons and with MboI digestion [data not shown]). Sequencing 10 clones each from two control and two LBR-expressing amplicons verifies that the OR transcriptome is more complex in LBR+ OSNs. In both control amplicons, all 10 clones were identical, and the sequence of the cloned OR matches the digestion pattern. In the case of the LBR+ neurons, 10/10 and 9/10 clones of each amplicon were unique and different from each other. Moreover, the sequences of these clones did not match their digestion pattern, suggesting that these libraries are very complex and the observed distinct bands represent comigrating bands of similar size digested from a large number of different ORs. To verify this, we sequenced 96 independent colonies from a third LBR+ single-cell library and identified 46 different ORs from 11 chromosomes without any zonal restrictions (Table S3). Thus, LBR expression in OSNs violates the "one receptor per neuron" rule and induces coexpression of a large number of ORs. To exclude that multiple ORs are expressed in low levels also in control OSNs but are masked by the highly expressed chosen allele, we pooled equal volumes of the single-cell RT reaction from a control and an LBR+ neuron and performed degenerate PCR and digest. Although the OR amplicon from the control neuron dominates the reaction, the ectopically coexpressed ORs from the LBR-expressing neuron are still detectable upon digestion (Figure S6B).

For a non-PCR based confirmation for OR coexpression in LBR+ OSNs, we performed IF for ORs M50, M71, and C6 in tetO-LBR/tetO-MOR28 double transgenics. Most OSNs that retain detectable OR levels by IF are LBR negative; thus, in these OSNs, OR coexpression is extremely rare. To overcome this, we exploited the frequent expression of transgenic MOR28 in the LBR-expressing mice. IF in MOE sections from double transgenics revealed double-positive OSNs (Figure 7C), which are not detected in the absence of LBR, as previously shown (Fleischmann et al., 2008; Nguyen et al., 2007). Most likely, these OSNs are shutting down the endogenous OR in response to LBR expression while activating the decondensing transgenic OR.

The identity of the expressed OR allele instructs the targeting of like neurons to a single glomerulus (Mombaerts, 2006). For this reason, we examined the targeting of neurons expressing the P2-IRES-τLacZ allele in LBR transgenics by IF for β-gal in olfactory bulb sections. β-gal protein is stable in the axons long after the cytoplasmic signal has faded (Figure S6D); thus, we can use this approach to examine the targeting consequences of LBR expression. In control mice, the β-gal-positive fibers coalesce in distinct glomeruli (Figure 7D), with very few axons targeting wrong glomeruli (extreme example shown in Figure S6C). However, upon LBR expression, β-gal-positive fibers extend to an extraordinary number of glomeruli (~30 per hemisphere per mouse). We detected extra distinct glomeruli and stray fibers both near wild-type P2 glomeruli and in ectopic positions in the bulb (Figures 7D and S6C).

DISCUSSION

We examined the role of nuclear architecture in monogenic OR expression. Using a complex OR-specific DNA FISH probe, we showed that OR genes converge into approximately five distinct and seemingly exclusive foci surrounding the PH core of the OSN nucleus. These foci contain frequently superimposed OR loci from the same chromosome and optically discrete OR clusters from different chromosomes. The OR allele transcribed in each OSN is absent from these foci. Although low-frequency interactions between OR clusters from chromosome 7 occur in embryonic liver and brain (Simonis et al., 2006), the widespread and differentiation-dependent interchromosomal aggregation and focal organization of the whole-OR subgenome may be unique to the OSN lineage. Thus, our experiments suggest that a primary epigenetic signature is reinforced by secondary and tertiary repressive organization: intrachromosomal compaction and interchromosomal aggregation of OR genes in OSNs. The importance of this elaborate arrangement is shown by the disruption of these aggregates, which results in violation of monogenic OR transcription and coexpression of a large number of ORs.

LBR and PH as Organizers of OR Aggregation

A loss-of-function LBR mutation results in ectopic OR aggregation in basal and sustentacular cells. Conversely, LBR expression in OSNs reverses the nuclear morphology and disrupts OR foci. Thus, regulation of LBR expression governs the spatial aggregation of OR genes in the MOE. LBR could act directly on ORs (through binding to HP1) and indirectly by recruiting pericentromeric heterochromatin to the nuclear envelope. ORs were not recruited to the nuclear envelope as efficiently as PH. The smaller size of OR clusters and their genomic embedding in euchromatin might make them less mobile than the acrocentric PH, which is robustly recruited to the nuclear periphery. Moreover, gene relocation to the nuclear envelope requires cell division (Zullo et al., 2012), which does not occur in OSNs. In any case, in wild-type OSNs, PH could provide a platform on which OR aggregates are formed upon LBR downregulation, and in LBR+ OSNs, PH relocation might help to untangle OR aggregates. The final biochemical outcome of this rearrangement is decompaction of OR heterochromatin, demonstrated by reduction of LAC values in SXT and increased DNaseI sensitivity.

Nonspecific effects of ectopic LBR expression cannot be excluded, although most non-OR genes are unaffected by ectopic LBR expression. Genes known or suspected to activate OR expression, like *Emx2*, *Lhx2*, and *Ebf* family members (Fuss and Ray, 2009), are either upregulated or unaffected by LBR expression (Figure S5A), making secondary effects an unlikely cause of OR downregulation. Moreover, LBR's weak enzymatic activity, which produces ergosterol, should not participate in OR regulation, as the Ichthyosis mouse does not have OR expression deficits. Furthermore, the enzymes that produce the substrate for LBR are both expressed at very low levels in OSNs (data not shown); thus, LBR is not the rate-limiting enzyme in this pathway, and its upregulation would not affect ergosterol levels.

Spatial Regulation of OR Expression

The fact that disruption of OR aggregation results in coexpression of multiple OR genes indicates that this organization is critical for the effective silencing of the nonchosen OR alleles in each OSN. It also implies that the heterochromatic marks found on ORs, which remain enriched on these loci upon LBR induction, are not sufficient to prevent basal transcription in the absence of higher-order folding of these chromatin regions. As in the phenomenon of transcriptional squelching, however (Gill and Ptashne, 1988), we made the counterintuitive observation that LBR induction in OSNs causes a significant overall reduction of OR transcription while allowing the coexpression of multiple alleles. This suggests that the process of OR choice is conceptually more complicated than, for example, the regulation of the tetO MOR28 transgene, and the extreme number of OR alleles might be a contributing factor. We propose that the unprecedented number of genes that share similar transcription factor binding motifs (Clowney et al., 2011) makes the effective cloaking of most of these alleles imperative for the high-level transcription of one allele. Thus, the heterochromatinization of most OR loci and their aggregation into large nuclear foci not only assures their effective silencing, but also conceals thousands of transcription factor binding sites that could sequester activating proteins from the chosen allele. Finally, the identification of multiple ORs in each LBR+ neuron may reflect a continuous switching process (Shykind et al., 2004) caused by the downregulation of the initially chosen OR and the inability to make a new, productive OR choice.

Genomic competition may not be the only reason for OR downregulation upon LBR expression. An equally elaborate network of interchromosomal interactions could be involved in the activation of a single OR allele. Consequently, escape from the heterochromatic foci might not be sufficient for activated OR transcription. The OR gene might also need to be repositioned to a specialized, transcription-competent interchromosomal hub, as is the case for IFNβ activation (Apostolou and Thanos, 2008). Consistent with this is the fact that the active OR allele is often found adjacent to the heterochromatic foci. This could imply that OR aggregation not only silences OR alleles, but also organizes some of them—probably those located on the periphery of foci—for activation. Poising or organizing aggregated ORs for future activation may provide a reason behind the selectivity of these foci for OR sequences. Thus, a nuclear overhaul induced by LBR expression would also disrupt activating interactions between long-distance enhancers and the chosen OR allele, resulting in OR downregulation. The observation that LBR expression disrupts the *trans* interactions between H and ORs is consistent with such a model. Although there is no genetic evidence for the requirement of simple *trans* interactions for OR transcription (Khan et al., 2011), a more elaborate network of interchromosomal interactions might govern OR activation, as is the case for OR silencing.

Nuclear Reorganization in Development

Differences in nuclear topology can be seen in many sensory epithelia (data not shown), and regulation of LBR expression may orchestrate some of them. Although reorganization of the nucleus might serve additional functions (Solovei et al., 2009), it could be critical for the execution of tissue-specific differentiation modules and may permanently lock in gene expression programs as they occur. Thus, at the highest level of chromatin organization, the epigenetic "landscape" becomes a physical landscape where particular genes and regulatory sequences are hidden or exposed in accordance with the cell type and function. Future experiments will reveal whether spatial regulatory mechanisms similar to the ones described here apply to less extreme developmental decisions that do not involve choosing one out of a thousand alleles.

EXPERIMENTAL PROCEDURES

Mice

Mice were housed under standard conditions in accordance with IACUC regulations and as described previously (Magklara et al., 2011). RNA FISH experiments were performed on postnatal day 6 (p6)–p10 animals. DNA FISH experiments shown here were performed on p14–p21 animals, and staining patterns were confirmed in younger (p7) and older (6 week) animals. IF, X-gal, sorting, RNA-seq, SXT, and biochemical experiments were performed in 4- to 8-week-old animals. For the construction of the tetO-LBR-IRES-GFP mouse and strains used in this paper, see the Extended Experimental Procedures.

Captured DNA FISH Probe Construction and Microarray Analysis

Captured DNA FISH probe construction and microarray analysis are described in schematic Figure 1A and detailed in the Extended Experimental Procedures and Table S1.

DNA FISH, Immuno-DNA FISH

DNA FISH experiments were performed as described previously (Lomvardas et al., 2006) with modifications described in the Extended Experimental Procedures and Tables S4 and S5.

Microscopy and Image Analysis

Confocal images were collected on a Zeiss LSM700. Channels have been pseudocolored here for consistency and visibility. Details can be found in the Extended Experimental Procedures.

SXT

Neurons were dissociated using papain dissolved in neurobasal A medium supplemented with HEPES, glutamine, and methylcellulose for 30–45 min, after which the reaction was stopped with addition of albumin. Cells were washed, filtered, loaded into capillaries, and imaged as described previously (Uchida et al., 2009). Statistical analyses were carried out using the Amira software package (Mercury Computer Systems).

Immunostaining and Antibodies

IF was performed under standard conditions on MOE cryosections; antibodies used are described in Table S5. LBR IF was performed with a custom antibody against mouse LBR (Olins et al., 2009). See also the Extended Experimental Procedures.

DNase Assay and Native ChIP

DNase assay and native ChIP were performed as described previously (Magklara et al., 2011). See also Table S6.

4C

4C was performed as described previously (Lomvardas et al., 2006). After inverse PCR, products were analyzed for enrichment by qPCR.

Expression Analysis

For Figure 6B, neurons where sorted and RNA extracted as described previously (Magklara et al., 2011). qRT-PCR primer sets are listed in Table S6. For RNA FISH, RNA-seq, X-gal staining, and single-cell RT-PCR analysis, see the Extended Experimental Procedures.

ACCESSION NUMBERS

Microarray analysis of panOR probe has been deposited in GEO under accession GSE38488.

SUPPLEMENTAL INFORMATION

Supplemental Information includes Extended Experimental Procedures, six figures, six tables, and four movies and can be found with this article online at http://dx.doi.org/10.1016/j.cell.2012.09.043.

ACKNOWLEDGMENTS

We would like to thank Dr. Nicholas Ryba for the Gγ8 tTA transgenic mice; Drs. Monica Zwerger and Harald Herrmann for the anti-LBR antibody; David Lyons and Drs. Richard Axel, Keith Yamamoto, and David Agard for input and suggestions; and Dr. Nirao Shah and the Lomvardas lab for critical reading of the manuscript. Also, we are grateful to Dr. Allan Basbaum for making the Shidduch between S.L. and C.A.L. E.J.C. and E.C.M.-P. are supported by fellowships from the National Science Foundation (NSF GRFP). This project was funded by the Roadmap for Epigenomics grant 5R01DA030320-02 and the McKnight Endowment for Neurosciences. National Center for X-Ray Tomography is funded by grants from the National Center for Research Resources (5P41RR019664-08) and the National Institute of General Medical Sciences (8 P41 GM103445-08) from the National Institutes of Health and US Department of Energy, Office of Biological and Environmental Research (DE-AC02-05CH11231). G.B. is a Pew scholar and is supported, in part, by NIH grant 5R01MH086920.

Received: January 19, 2012
Revised: May 18, 2012
Accepted: September 26, 2012
Published: November 8, 2012

REFERENCES

Albert, T.J., Molla, M.N., Muzny, D.M., Nazareth, L., Wheeler, D., Song, X., Richmond, T.A., Middle, C.M., Rodesch, M.J., Packard, C.J., et al. (2007). Direct selection of human genomic loci by microarray hybridization. Nat. Methods *4*, 903–905.

Apostolou, E., and Thanos, D. (2008). Virus Infection Induces NF-kappaB-dependent interchromosomal associations mediating monoallelic IFN-beta gene expression. Cell *134*, 85–96.

Buck, L., and Axel, R. (1991). A novel multigene family may encode odorant receptors: a molecular basis for odor recognition. Cell *65*, 175–187.

Chess, A., Simon, I., Cedar, H., and Axel, R. (1994). Allelic inactivation regulates olfactory receptor gene expression. Cell *78*, 823–834.

Clowney, E.J., Magklara, A., Colquitt, B.M., Pathak, N., Lane, R.P., and Lomvardas, S. (2011). High-throughput mapping of the promoters of the mouse olfactory receptor genes reveals a new type of mammalian promoter and provides insight into olfactory receptor gene regulation. Genome Res. *21*, 1249–1259.

de Wit, E., and de Laat, W. (2012). A decade of 3C technologies: insights into nuclear organization. Genes Dev. *26*, 11–24.

Eskiw, C.H., Cope, N.F., Clay, I., Schoenfelder, S., Nagano, T., and Fraser, P. (2010). Transcription factories and nuclear organization of the genome. Cold Spring Harb. Symp. Quant. Biol. *75*, 501–506.

Fleischmann, A., Shykind, B.M., Sosulski, D.L., Franks, K.M., Glinka, M.E., Mei, D.F., Sun, Y., Kirkland, J., Mendelsohn, M., Albers, M.W., and Axel, R. (2008). Mice with a "monoclonal nose": perturbations in an olfactory map impair odor discrimination. Neuron *60*, 1068–1081.

Fraser, P., and Bickmore, W. (2007). Nuclear organization of the genome and the potential for gene regulation. Nature *447*, 413–417.

Fuss, S.H., and Ray, A. (2009). Mechanisms of odorant receptor gene choice in Drosophila and vertebrates. Mol. Cell. Neurosci. *41*, 101–112.

Garrick, D., Fiering, S., Martin, D.I., and Whitelaw, E. (1998). Repeat-induced gene silencing in mammals. Nat. Genet. *18*, 56–59.

Gill, G., and Ptashne, M. (1988). Negative effect of the transcriptional activator GAL4. Nature *334*, 721–724.

Glusman, G., Yanai, I., Rubin, I., and Lancet, D. (2001). The complete human olfactory subgenome. Genome Res. *11*, 685–702.

Goldowitz, D., and Mullen, R.J. (1982). Nuclear morphology of ichthyosis mutant mice as a cell marker in chimeric brain. Dev. Biol. *89*, 261–267.

Hoffmann, K., Dreger, C.K., Olins, A.L., Olins, D.E., Shultz, L.D., Lucke, B., Karl, H., Kaps, R., Müller, D., Vayá, A., et al. (2002). Mutations in the gene encoding the lamin B receptor produce an altered nuclear morphology in granulocytes (Pelger-Huët anomaly). Nat. Genet. *31*, 410–414.

Imai, T., Sakano, H., and Vosshall, L.B. (2010). Topographic mapping—the olfactory system. Cold Spring Harb. Perspect. Biol. *2*, a001776.

Khan, M., Vaes, E., and Mombaerts, P. (2011). Regulation of the probability of mouse odorant receptor gene choice. Cell *147*, 907–921.

Liu, Z., Scannell, D.R., Eisen, M.B., and Tjian, R. (2011). Control of embryonic stem cell lineage commitment by core promoter factor, TAF3. Cell *146*, 720–731.

Lomvardas, S., Barnea, G., Pisapia, D.J., Mendelsohn, M., Kirkland, J., and Axel, R. (2006). Interchromosomal interactions and olfactory receptor choice. Cell *126*, 403–413.

Magklara, A., Yen, A., Colquitt, B.M., Clowney, E.J., Allen, W., Markenscoff-Papadimitriou, E., Evans, Z.A., Kheradpour, P., Mountoufaris, G., Carey, C., et al. (2011). An epigenetic signature for monoallelic olfactory receptor expression. Cell *145*, 555–570.

McDermott, G., Le Gros, M.A., Knoechel, C.G., Uchida, M., and Larabell, C.A. (2009). Soft X-ray tomography and cryogenic light microscopy: the cool combination in cellular imaging. Trends Cell Biol. *19*, 587–595.

Mombaerts, P. (2006). Axonal wiring in the mouse olfactory system. Annu. Rev. Cell Dev. Biol. *22*, 713–737.

Montavon, T., Soshnikova, N., Mascrez, B., Joye, E., Thevenet, L., Splinter, E., de Laat, W., Spitz, F., and Duboule, D. (2011). A regulatory archipelago controls Hox genes transcription in digits. Cell *147*, 1132–1145.

Nguyen, M.Q., Zhou, Z., Marks, C.A., Ryba, N.J., and Belluscio, L. (2007). Prominent roles for odorant receptor coding sequences in allelic exclusion. Cell *131*, 1009–1017.

Okada, Y., Suzuki, T., Sunden, Y., Orba, Y., Kose, S., Imamoto, N., Takahashi, H., Tanaka, S., Hall, W.W., Nagashima, K., and Sawa, H. (2005). Dissociation of heterochromatin protein 1 from lamin B receptor induced by human polyomavirus agnoprotein: role in nuclear egress of viral particles. EMBO Rep. *6*, 452–457.

Olins, A.L., Hoang, T.V., Zwerger, M., Herrmann, H., Zentgraf, H., Noegel, A.A., Karakesisoglou, I., Hodzic, D., and Olins, D.E. (2009). The LINC-less granulocyte nucleus. Eur. J. Cell Biol. *88*, 203–214.

Peric-Hupkes, D., Meuleman, W., Pagie, L., Bruggeman, S.W., Solovei, I., Brugman, W., Gräf, S., Flicek, P., Kerkhoven, R.M., van Lohuizen, M., et al. (2010). Molecular maps of the reorganization of genome-nuclear lamina interactions during differentiation. Mol. Cell *38*, 603–613.

Peric-Hupkes, D., and van Steensel, B. (2010). Role of the nuclear lamina in genome organization and gene expression. Cold Spring Harb. Symp. Quant. Biol. *75*, 517–524.

Pyrpasopoulou, A., Meier, J., Maison, C., Simos, G., and Georgatos, S.D. (1996). The lamin B receptor (LBR) provides essential chromatin docking sites at the nuclear envelope. EMBO J. *15*, 7108–7119.

Shykind, B.M., Rohani, S.C., O'Donnell, S., Nemes, A., Mendelsohn, M., Sun, Y., Axel, R., and Barnea, G. (2004). Gene switching and the stability of odorant receptor gene choice. Cell *117*, 801–815.

Simonis, M., Klous, P., Splinter, E., Moshkin, Y., Willemsen, R., de Wit, E., van Steensel, B., and de Laat, W. (2006). Nuclear organization of active and inactive chromatin domains uncovered by chromosome conformation capture-on-chip (4C). Nat. Genet. *38*, 1348–1354.

Solovei, I., Kreysing, M., Lanctôt, C., Kösem, S., Peichl, L., Cremer, T., Guck, J., and Joffe, B. (2009). Nuclear architecture of rod photoreceptor cells adapts to vision in mammalian evolution. Cell *137*, 356–368.

Uchida, M., McDermott, G., Wetzler, M., Le Gros, M.A., Myllys, M., Knoechel, C., Barron, A.E., and Larabell, C.A. (2009). Soft X-ray tomography of phenotypic switching and the cellular response to antifungal peptoids in Candida albicans. Proc. Natl. Acad. Sci. USA *106*, 19375–19380.

Zacharias, H. (1995). Emil Heitz (1892-1965): chloroplasts, heterochromatin, and polytene chromosomes. Genetics *141*, 7–14.

Zullo, J.M., Demarco, I.A., Piqué-Regi, R., Gaffney, D.J., Epstein, C.B., Spooner, C.J., Luperchio, T.R., Bernstein, B.E., Pritchard, J.K., Reddy, K.L., and Singh, H. (2012). DNA sequence-dependent compartmentalization and silencing of chromatin at the nuclear lamina. Cell *149*, 1474–1487.